Tropical Storm Development and Decay: Sensitivity to Surface Boundary Conditions

ROBERT E. TULEYA

Geophysical Fluid Dynamics Laboratory/National Oceanic and Atmospheric Administration, Princeton, New Jersey

(Manuscript received 7 June 1993, in final form 13 August 1993)

ABSTRACT

Hurricane models have rarely been used to investigate the observational fact that tropical disturbances seldom form, develop, or intensify over land. Furthermore, rather ad hoc assumptions have been made when modeling landfall. The general consensus is that energy supplied primarily through surface fluxes is necessary for tropical cyclone development and maintenance. In the past, rather a priori assumptions have been made such as the elimination of surface sensible and latent heat fluxes over land or the reduction of surface land temperature. By incorporating an improved version of the Geophysical Fluid Dynamics Laboratory (GFDL) tropical cyclone model with diurnal radiation and a bulk subsurface layer with explicit prediction of land temperature, a series of experiments was performed to test the sensitivity of surface boundary conditions to tropical cyclone development and decay at landfall.

A triply nested version of the GFDL model was used in an idealized setting in which a tropical disturbance, taken from the incipient stage of Gloria (1985), was superposed on a uniform easterly flow of 5 m s^{-1}. A control case was performed for ocean conditions of fixed 302-K SST in which the initial disturbance of about 998 hPa developed to a quasi-steady state of 955 hPa after one day of integration. Using identical atmospheric conditions, a series of experiments was performed in which the underlying land surface was specified with different values of thermal property, roughness, and wetness. By systematically changing the thermal property (i.e., heat capacity and conductivity) of the subsurface from values typical of a mixed-layer ocean to those of land, a progressively weaker tropical system was observed. It was found that the initial disturbance over land failed to intensify below 985 hPa, even when evaporation was specified at the potential rate. The reduction of evaporation over land, caused primarily by the reduction of surface land temperature near the storm core, was responsible for the inability of the tropical disturbance to develop to any large extent. Under land conditions, the known positive feedback between storm surface winds and surface evaporation was severely disrupted.

In sensitivity experiments analogous to the all-land cases, a series of landfall simulations were performed in which land conditions were specified for a region of the domain so that a strong mature tropical cyclone similar to the ocean control case encountered land. Again as in the all-land case, the demise of the landfalling storm takes place due to the suppression of the potential evaporation and the associated reduction of surface temperatures beneath the landfalling cyclone. Even when evaporation was prescribed at the potential rate, a realistic rapid filling (36 hPa in 12 h) ensued despite the idealized nature of the simulations. Although not critical for decay, it was found that surface roughness and reduced relative wetness do enhance decay at landfall.

1. Introduction

Hurricane modeling efforts have recently been concerned with behavior of tropical cyclones over the open ocean and the associated perplexing problems of convective parameterization, track movement, and vortex–flow interaction. Over the past decade, little has been investigated about the observational fact that tropical disturbances seldom form, develop, or intensify over land. Early general circulation models were capable of developing disturbances in the tropics over land and sea (Manabe and Smagorinsky 1967; Manabe et al. 1970), but these and more recent studies (e.g., Bengtsson et al. 1982; Krishnamurti et al. 1989; Broccoli and Manabe 1990) have been handicapped by questions of resolution and physical reality (McBride 1984; Evans 1992). On the other hand, early hurricane modeling efforts discovered the acute sensitivity of hurricane development to surface energy fluxes mainly through alterations of the drag coefficients of heat, moisture, and momentum (e.g., Ooyama 1969; Rosenthal 1971). These studies revealed that tropical cyclones failed to develop when drag coefficients were reduced to relatively small values. Subsequent studies of Tuleya and Kurihara (1978) differentiated between the relative roles of evaporation cutoff and increased friction at least as far as landfall was concerned.

Through the aforementioned and subsequent modeling studies, as well as the classic observational work of Miller (1964), a general consensus of understanding has developed that energy supply primarily through surface fluxes is necessary for tropical cyclone development and maintenance. The detailed scenario on how this energy supply is retarded over land has not been modeled or investigated. In the past, rather a priori

Corresponding author address: Dr. Robert E. Tuleya, NOAA/GFDL, Princeton University, P.O. Box 308, Princeton, NJ 08542.

assumptions have been made. For example, no surface sensible nor latent heat fluxes over land are assumed in the operational National Meteorological Center (NMC) quasi-Langrangian model (Mathur 1991) while fixed reduced surface temperature over land, T_L, was assumed in research studies of landfall (Tuleya et al. 1984). To accurately model the interactions of the hurricane with any underlying surface, one must account for the energy fluxes at the surface, including longwave and shortwave radiative effects. For the most part, hurricane modeling has ignored this additional complexity with radiational effects being disregarded. This radiative assumption may be acceptable over oceans but necessitates further simplifying assumptions over land.

The impact of the underlying surface on a landfalling tropical cyclone has drawn more attention. Important observational studies have been performed when hurricanes come ashore, including those of Miller (1964), Powell (1987), and Bluestein and Hazen (1989). In addition, the landfall question has been addressed by modeling efforts (e.g., Tuleya and Kurihara 1978). These studies reveal that the elimination of surface evaporation is critical to landfall decay. Also, decay was affected by downslope, topographically induced subsidence (Bender et al. 1985, 1987). These studies were again subject to the aforementioned assumptions.

Using an idealized framework, this study will attempt to examine and extend earlier research results by relaxing some of the more pertinent assumptions by using more realistic physical parameterizations of land surface processes. By incorporating an improved version of the Geophysical Fluid Dynamics Laboratory (GFDL) tropical cyclone model with diurnal radiation and a bulk subsurface layer with explicit prediction of T_L, a series of experiments was performed to test the sensitivity of surface boundary conditions to tropical cyclone development and landfall. The question of why tropical disturbances seldom form and inevitably decay upon landfall will be answered from a more physically realistic basis. The mechanism that causes the apparent cool pool of air beneath the tropical circulations over land, especially during the day, will be revealed, including the relative role of the cloud canopy in this cooling. The relative roles of surface wetness, surface roughness, subsurface thermal property, and diurnal variation in retarding growth of a tropical disturbance over land will also be examined.

The modifications and improvements made to the GFDL model together with the experimental design will be described in section 2. The impact of the underlying surface on the intensity of a developing and a landfalling tropical disturbance will be discussed in sections 3 and 4, respectively. A summary of the results of these idealized experiments will be presented in section 5.

2. Experimental design

To increase the forecast skill of the GFDL multiply nested movable mesh model (MMM), physical improvements have recently been incorporated (Kurihara et al. 1993). The more relevant improvements include the Schwarzkopf and Fels (1991) infrared and Lacis and Hansen (1974) solar radiation parameterizations with diurnal variation and cloud specification; the use of vegetation type to specify the surface roughness length, evaporation efficiency, and surface albedo; and the inclusion of a bulk subsurface layer with explicit prediction of T_L. For the present idealized experiments, the roughness length, evaporation efficiency, and surface albedo were specified, not set according to vegetation type. These changes will be covered in more detail in this section together with the design of experiments.

a. Implementation of a bulk surface temperature prediction scheme into the GFDL model

To provide physically realistic forecasts over land, a bulk subsurface layer was added to the GFDL MMM. Following Deardorff (1978), one can assume a surface energy balance:

$$\sigma T_L^4 + H + \mathrm{LE} - (S + F\downarrow) = G \qquad (1.1)$$

$$H = \rho c_p C_e V(T_L - \theta_{va}) \qquad (1.2)$$

$$\mathrm{LE} = (\mathrm{WET})\rho L C_e V[R_s(T_L) - R_a],$$

where G is the net ground surface heat flux, H is the surface sensible heat flux, LE is the surface evaporative heat flux, σT_L^4 is the emission from the earth's surface, and $(S + F\downarrow)$ is the net downward radiative surface flux. In the preceding formulations the drag coefficient of heat and moisture C_e is calculated in the Monin–Obukhov framework in a manner similar to Kurihara and Tuleya (1974), where V is the low-level wind speed; θ_{va} is the virtual potential temperature of the surface air; WET is the wetness coefficient; R_s and R_a are the mixing ratios of the saturated surface land temperature and of the low-level air, respectively; L is the latent heat of condensation; ρ is the density of the low-level air; and c_p is the specific heat of air. One may then obtain the ground surface temperature through the tendency equation:

$$\frac{\partial T_L}{\partial t} = \frac{-\sigma T_L^4 - H - \mathrm{LE} + (S + F\downarrow)}{\rho_s c_s d} - c(T_L - T_{\mathrm{gref}}), \qquad (1.3)$$

where $\rho_s c_s$ is the soil heat capacity and d is the damping depth $(\tau\lambda/\rho_s c_s \pi)^{1/2}$ where λ is the thermal conductivity of soil and τ is the period of forcing (24 h) and $c = 2\pi/\tau$. The last term in (1.3) is used to "force–restore" the surface temperature to some reference value (i.e., 302 K) and avoid spurious trends. Deardorf (1978) found

that this method could adequately simulate the thermal evolution of a more complicated multiple-level ground model. The effects of the subsurface layer on the surface temperature may be combined into one parameter, referred to by Sellers (1967) as the thermal property TP, which may be defined as the square root of the product of the heat capacity and the thermal conductivity. For most experiments in the present study the thermal property was specified as 0.05 cal cm^{-2} K^{-1} $s^{-1/2}$, corresponding to a soil heat capacity of 0.5 cal cm^{-3} K^{-1} and a thermal conductivity of 0.005 cal cm^{-1} K^{-1} s^{-1} over land. For all but one experiment, c was set to 0 for the relatively short two- to four-day integration time with little detrimental effect.

b. Implementation of radiation

As mentioned, the Schwarzkopf and Fels (1991) infrared and Lacis and Hansen (1974) solar radiation parameterizations were incorporated into the MMM with a radiative calculation being performed every 10 min, while at intermediate times the net radiative fluxes are held constant. The MMM includes interactive radiational effects of clouds and was normally run in diurnal varying mode but has the option to run for diurnally averaged conditions. As in Tuleya (1988), clouds are specified simply where model condensation occurs. Additional options also exist to run with fixed, climatological specified, seasonally averaged, zonally fixed cloud distributions (London 1957). One experiment was run under these special circumstances to evaluate the effects of cloud interaction and diurnal variability in the tropical cyclone development problem. The radiative properties of clouds were specified in a similar manner to Kurihara and Tuleya (1981) with a spectrum of cloud depths possible. In the present idealized study the surface albedo was specified to be 0.20 over land and 0.06 over water.

c. Initial conditions and experimental framework

The initial condition for the present experiments was based on an idealized state of the early stages of Hurricane Gloria on 22 September 1985. A specified vortex was superposed on a uniform easterly current of 5 m s^{-1} at 58°W in a domain spanning 10°S–45°N, 95°–40°W. The model initial condition had low-level maximum winds of 28 m s^{-1} with a central surface pressure of 996 hPa. A model control simulation was performed for four days in which ocean only conditions (i.e., fixed 302-K SST) were specified. This control experiment exhibited considerable cyclogenic behavior. Except for the aforementioned radiation package, the control simulation was identical to the control experiment of Bender et al. (1994). In these experiments an eighteen-level, triply nested version of the GFDL MMM was used with mesh resolutions of 1/6°, 1/3°, and 1° with corresponding mesh sizes of 81/3°, 142/3°, and 55°, respectively.

The model simulations of land conditions could be categorized into two types: 1) all-land and 2) landfall. For all sensitivity experiments described the initial atmospheric condition was identical with an initial time at 0000 UTC (2000 LST). In the all-land type simulation, values of albedo, roughness, thermal property, and wetness were specified uniformly throughout the 55° × 55° domain. For most experiments the values of albedo and thermal property were specified at 0.2 and 0.05 cal cm^{-2} K^{-1} $s^{-1/2}$, respectively. The roughness was set to 1 cm and the relative wetness was specified to allow evaporation at the potential rate; that is, WET = 1.0. The integrations were performed for a two-day period with cloud specification and diurnal varying radiation. For a series of four experiments, all-land conditions were specified except that the thermal property was specified at different amounts to simulate a transition from typical land conditions to those with thermal property near that of a mixed-layer ocean. In another series of experiments, the land wetness, roughness, and temperature formulation were varied. For one experiment the roughness coefficient was increased from 1 to 25 cm, probably a more realistic land value. In another experiment the wetness was set to 0.3 to test the sensitivity of the relative wetness. For all experiments except one the surface temperature was predicted as described above. For another sensitivity experiment, the surface temperature was specified at 302 K. In yet another experiment, the effects of cloud canopy and diurnal variation were tested by running a land case with no diurnal variability and zonally prescribed clouds. Table 1 (upper) summarizes the all-land experiments.

Four landfall simulations were performed in which land conditions were specified west of 73°W. The atmospheric conditions were identical to those before and the model was integrated for four days. In these experiments landfall occurred at about 72 h of the integration (2000 LST). As in the all-land cases, one experiment was performed for potentially wet conditions with a roughness length of 1 cm and land surface temperature predicted. In a second experiment, the relative wetness was specified as 0.3. In a third experiment the roughness length was increased to 25 cm, while in a fourth experiment land conditions were specified, except that the land temperature was fixed at 302 K. In all four of these simulations the surface albedo was set at 0.20 and thermal property of 0.05 cal cm^{-2} K^{-1} $s^{-1/2}$. As previously mentioned, a control ocean simulation was performed for four days. Table 1 (lower) summarizes the landfall experiments.

3. Impact of surface conditions on a developing case

a. Effect of thermal property

A series of experiments were performed in which land conditions were specified except the thermal

property was varied from typical soil values of 0.05 to 6 cal cm^{-2} K^{-1} $s^{-1/2}$, which is considered to be an approximate mixed-layer ocean value (Sellers 1967). These experiments were carried out for potentially wet, relatively smooth surface roughness of 1 cm. Figure 1 displays the time history of minimum surface pressure from these experiments as well as the ocean control case. One sees a progression from intense development (a central pressure of 950 hPa) for a thermal property of 6 cal cm^{-2} K^{-1} $s^{-1/2}$, similar to the ocean control case, to little development (985 hPa) for the typical soil case (TP = 0.05 cal cm^{-2} K^{-1} $s^{-1/2}$). Little development ensued despite the favorable conditions of high vorticity and wet and relatively smooth surface conditions. In addition, a systematic phase change of the maximum domain-averaged precipitation (not shown) took place from an early morning maximum in the ocean control and high thermal property experiments to afternoon and evening for the experiment with a thermal property typical of soil. For soil conditions, a much greater diurnal amplitude of evaporative and sensible heat fluxes as well as surface and low-level temperatures was observed. As long as the thermal property was specified at high values (6 cal cm^{-2} K^{-1} $s^{-1/2}$) little impact was seen in such basic quantities as storm intensity and domain-averaged precipitation and evaporation when changing the albedo from land values (0.20) to ocean values (0.06).

These experiments indicate that even for potentially wet conditions, dynamically favorable atmospheric conditions failed to develop a tropical storm to any significant degree when subjected to a realistic soil subsurface. As the thermal property was allowed to increase toward values more typical of a mixed-layer ocean, a development not unlike that of the ocean control with fixed surface temperatures ensued. These results are consistent with the rather remarkable prototype GCM results of Manabe and Smagorinsky (1967) and Manabe et al. (1970), which indicated that tropical disturbances rarely developed low pressure centers for wet land conditions with zero heat capacity.

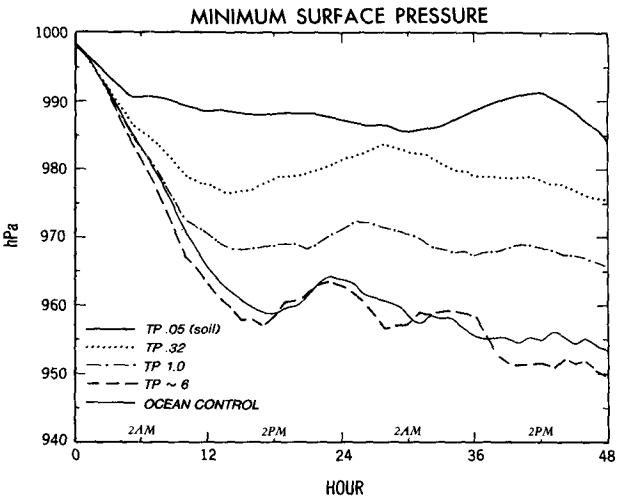

FIG. 1. Tropical storm evolution in a series of experiments with different heat capacity and conductivity of a bulk subsurface layer are contrasted with that of an ocean control case in which a fixed surface temperature of 302 K (infinite heat capacity) was assumed. The thermal property TP, defined as the square root of the product of the heat capacity and the thermal conductivity, is gradually changed from soil conditions (0.05 cal cm^{-2} K^{-1} $s^{-1/2}$) to mixed-layer ocean conditions (6 cal cm^{-2} K^{-1} $s^{-1/2}$).

b. *Effect of roughness, wetness, and T_L formulation*

In this series of experiments, surface roughness, wetness, and surface temperature formulation were separately varied from the all-land case with TP = 0.05 cal cm^{-2} K^{-1} $s^{-1/2}$ from section 3a. The results are

TABLE 1. List of experiments performed.

	z_0 (cm)	WET	Thermal property	Surface albedo	T_L formulation	Diurnal variability	Clouds
Thermal property experiments	1	1.0	0.05	0.20	predicted	yes	variable
	1	1.0	0.32	0.20	predicted	yes	variable
	1	1.0	1.0	0.20	predicted	yes	variable
	1	1.0	6.0	0.20	predicted	yes	variable
		1.0					
Wetness, roughness, fixed T_L experiments	1	0.3	0.05	0.20	predicted	yes	variable
	25	1.0	0.05	0.20	predicted	yes	variable
	1	1 0	0.05	0.20	302 K	yes	variable
	1	1.0	0.05	0.20	predicted	no	fixed zonal
Ocean control	Charnock's formulation	1.0	∞	0.06	302 K	yes	variable
Landfall experiments (land values)	1	1.0	0.05	0.20	predicted	yes	variable
	1	0.3	0.05	0.20	predicted	yes	variable
	25	1.0	0.05	0.20	predicted	yes	variable
	1	1.0	0.05	0.20	302 K	yes	variable

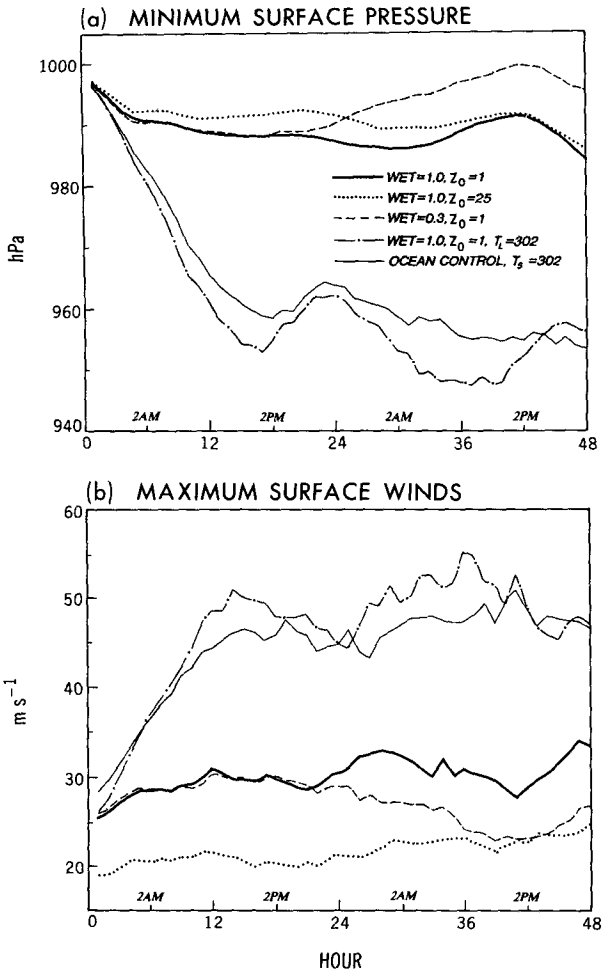

FIG. 2. (a) Minimum surface pressure and (b) maximum surface winds as a function of time for a series of experiments that are contrasted to an ocean control case. Surface wetness and roughness are separately altered in two experiments. In a third experiment, land conditions are specified except the surface land temperature is fixed at 302 K.

summarized in Fig. 2. To investigate the role of surface roughness, z_0 was increased from a relatively smooth value of 1 cm to perhaps a more typical value of 25 cm in an experiment with land conditions. The results indicate a rather small but systematic increase in the central surface pressure (<5 hPa) compared to the case of z_0 = 1 cm. The impact of the surface winds were, of course, more noticeable ranging from 5 to 10 m s^{-1}. At 24 h, for example, the maximum low-level winds are reduced from 28 to 20 m s^{-1}. The total kinetic energy is approximately the same, however, throughout the two-day period of these two experiments, indicating that this effect is rather shallow and confined primarily to the boundary layer.

In another experiment the role of the relative surface wetness was assessed by reducing the wetness from the potential rate, WET = 1, to a value of 0.3. In both idealized and realistic real data experiments, the prediction and verification of surface wetness is rather difficult with soil moisture not being a routinely observed quantity. Therefore this experiment tests the effects of the rather crude approximation of specifying relative wetness, rather than predicting it, at least as far as tropical development is concerned. One sees little apparent difference observed in the simulation (Fig. 2) until after sunrise more than 12 h after the initial time. It is then that the evaporation rate and sensible heat flux are affected and the case of WET = 0.3 becomes less intense than the potentially wet case. An intensity difference of about 5 m s^{-1} and 4 hPa is observed in the second day of integration between these two experiments. Nevertheless, these three experiments demonstrate that increased roughness and increased dryness are not necessary to explain lack of development. Development failed to occur even for the case of the rather smooth surface, z_0 = 1, where surface evaporation was set to the potential rate, WET = 1.

On the other hand, if T_L is fixed at the initial value of 302 K in another experiment, significant development ensues with central surface pressure lower and low-level winds higher than the ocean control case (Fig. 2). Even if roughness is increased with fixed T_L of 302 K (not shown), a similar surface pressure development ensues except the boundary-layer winds are somewhat retarded. It will be shown that the primary mechanism for land retardation of development is the reduction of land surface temperature near the storm core and the subsequent retardation of the surface evaporative heat fluxes.

c. *Reduction of surface energy flux and surface temperature*

The surface latent evaporative flux from the ocean is considered the primary energy source of a tropical cyclone. This has been recently reemphasized by Emanuel (1988). The 48-h accumulated sum of this quantity indicates a clear distinction between the ocean control case (Fig. 3, bottom) and the wetland case (Fig. 3, top) with z_0 = 1 cm. For the ocean control case there is a strong correlation between the maximum accumulated evaporative flux and the high winds along the storm track. This is indicative of the positive feedback process between surface evaporation and increased low-level wind. There is no indication of a similar feature in the land case, except perhaps an ill-defined broadening of the region greater than 2 × 10^7 J m^{-2} surrounding the land-based disturbance. The maximum evaporation rate in the ocean control is greater than 40 mm day^{-1} compared to a maximum in the land case of 25 mm day^{-1}. As will be seen later, the evaporation rate over land is strongly modulated by diurnal forcing with maximum values being often less than 10 mm day^{-1} at night.

The cause of this reduced evaporation is the development of a cool, relatively dry pool of air associated

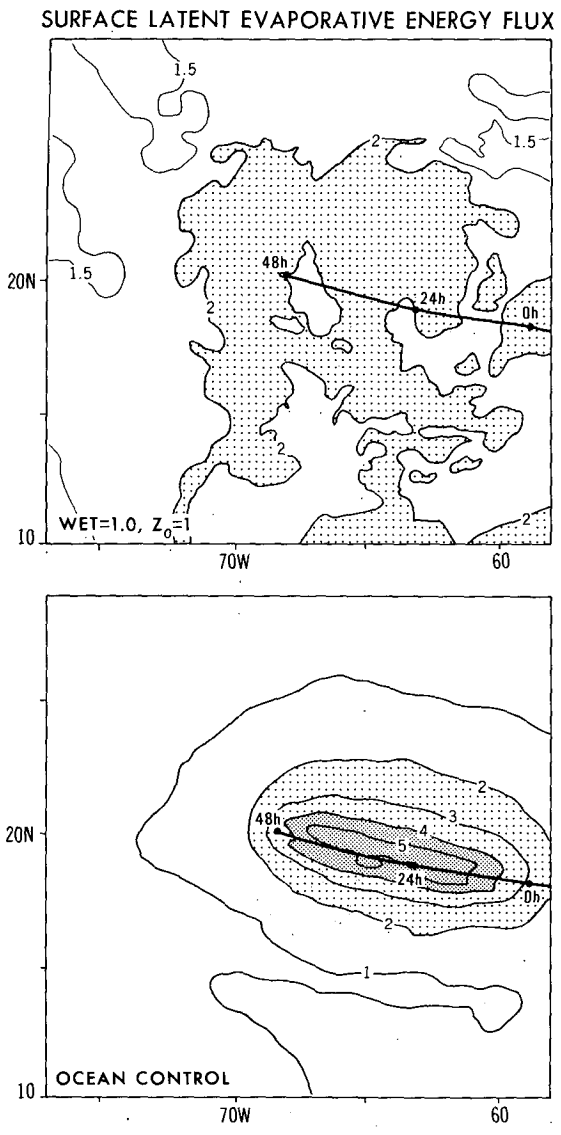

FIG. 3. Total accumulated surface latent evaporative energy flux for the experiment with evaporation set to the potential rate (i.e., WET = 1) and roughness length z_0 = 1 cm (top) and for the ocean control case with specified SST = 302 K (bottom). Units are 10^7 J m^{-2} for the 48-h integration period with storm track and 24-h position indicated for both experiments. Values greater than 2×10^7 J m^{-2} are shaded.

with cool ground temperatures near the disturbance core. This is a persistent feature for all cases with soil conditions although the case with WET = 1 and z_0 = 1 cm will be emphasized here. At 18 h (1400 LST) T_L is observed to be 298 K near the disturbance center (Fig. 4a) with maximum values of about 308 K in the surrounding regions. The large values in the surrounding relatively cloud-free regions were found to be near their highest at this time of large solar heating. Associated with this cool T_L is a corresponding surface air temperature minimum of 299 K and a dry region of less than 19 g kg^{-1} (Fig. 4b). This value of mixing ratio near the center compares with values greater than 23 g kg^{-1} in the ocean control case. The combination of the aforementioned thermal and moisture fields leads to a reduction of more than 12 K of low-level equivalent potential temperature θ_e of the land case compared to the ocean control (Figs. 4c,d). A minimum of θ_e of less than 348 K occurs near the disturbance center over land in contrast to a maximum greater than 360 K in the ocean case. It has been shown that high low-level θ_e is well correlated to surface energy input and therefore storm intensity. In the typical developing tropical cyclone over water the moist enthalpy of the incoming low-level air is increased by surface fluxes as it approaches the storm core leading to increased values of θ_e near the center (Hawkins and Imbembo 1976). As shown in Figs. 3 and 4, this energy input is highly impeded over land.

One can look at the time evolution of the surface temperatures and the tendency components of (1.3) at a point near the disturbance center and for one in the outer reaches, 640 km from the center (Fig. 5). Notice that the maximum temperature difference is for the daytime periods. A similar phenomenon was observed for the landfalling case of Alicia (1983) in a study by Bluestein and Hazen (1989). A look at the components of the surface temperature tendency indicates more evaporative cooling at night in the central storm region than in the surroundings. The relative effect of evaporative cooling is not as obvious during the day. On the other hand, the cloud canopy effect is evident below the disturbance region in the reduced values of net downward radiative flux ($S + F\downarrow$) relative to the surroundings during the day. At night this effect is reversed with more heating beneath the disturbance region attributable to trapping of outgoing longwave radiation. The impact of clouds is clearly shown by the rapid changes in net downward flux and evaporative cooling terms, especially during times of solar heating. Also note the positive sensible heat contribution near the disturbance center relative to the outer reaches. The sensible heat flux is directed downward near the center due to the presence of relatively warm air above the surface. Although not shown here, the sensible heat flux in the outer reaches in cloud-free areas and the sensible heat flux domain average, as well, are net upward during the period of solar heating, as one might expect.

d. Impact of the diurnal cycle and variable clouds

It was noticed from the energy components that clouds and the diurnal cycle have an obvious impact on the energy budget. To investigate the overall sensitivity of the disturbance intensity, as well as the hydrologic cycle, to cloud variation and the diurnal cycle, an experiment was performed without the diurnal cycle and for zonally fixed clouds. The same smooth, poten-

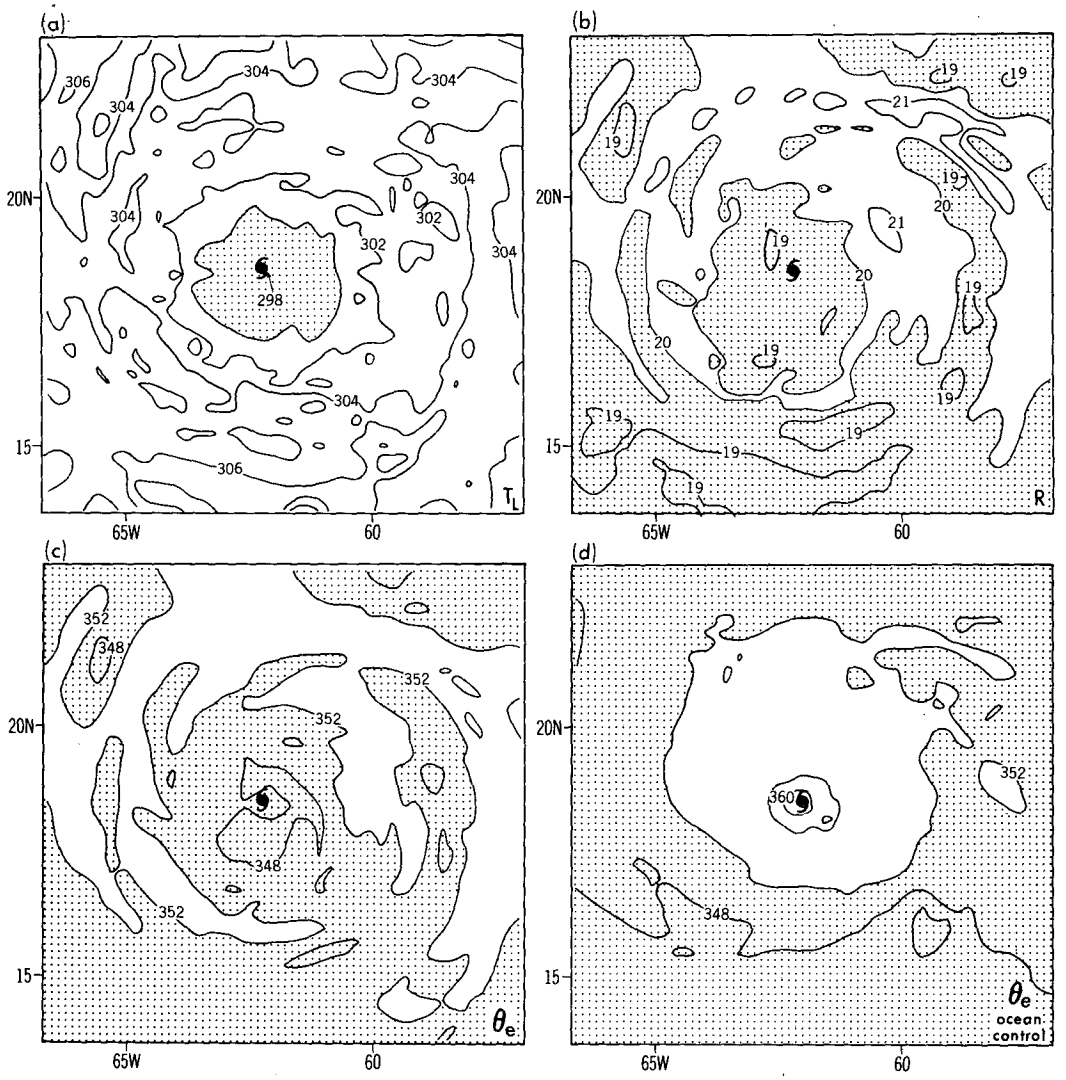

FIG. 4. (a) Composite distribution near and surrounding the disturbance of land temperature, (b) low-level mixing ratio, and (c) equivalent potential temperature for the case over land with evaporation at the potential rate at 18 h (1400 LST). For this case the roughness is set to 1 cm. (d) The corresponding distribution of equivalent potential temperature of the ocean control experiment is also shown. The shaded areas indicate relatively cool and/or dry areas.

tially wet land surface condition was used as previously. To ensure proper radiative balance, the force–restore method of (1.3) with $c = 2\pi/\tau$ was invoked. As indicated in Fig. 6a, the overall intensity of the developing system was the same as the diurnal and cloud-varying case with little significant development relative to the ocean control case. Notice that after an apparent one-day adjustment time the state of development is relatively constant. In contrast, this figure suggests a small diurnal variability with minimum intensity during the day and maximum intensity at night for the diurnally varying case over land. As opposed to the diurnally averaged, fixed clouds case, the maximum surface evaporation (Fig. 6b) has a distinct diurnal variation with maximum daytime values. But the maximum value during the daytime over the land is still considerably less than the maximum evaporation for the ocean control. Figure 6c displays the domain average precipitation for the diurnally averaged, fixed clouds case compared to the ocean control and diurnally varying, variable cloud land case. Within a few hours the domain average precipitation becomes quasi-steady, approximately, 3 mm day^{-1}, for the diurnally averaged, fixed cloud case. Compared to this, the other two cases display marked diurnal variability with the land case displaying maximum average precipitation during the midday and evening, at and after the time of maximum surface heating and evaporation, whereas the ocean control case indicates late evening and early morning precipitation. It is interesting that for the land

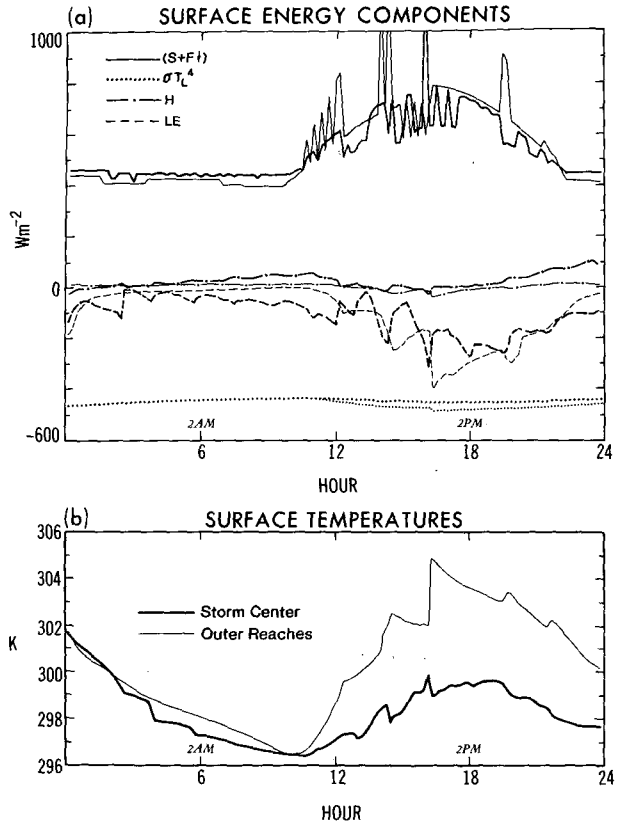

FIG. 5. (a) Surface energy flux components (W m^{-2} s^{-1}) for the first 24 h of the experiment with evaporation set to the potential rate (i.e., WET = 1) and roughness length z_0 = 1 cm. The net downward radiative flux, surface emission, sensible heat flux, and latent heat flux are indicated by solid, dotted, dashed–dotted, and dashed lines, respectively. The surface emission, sensible heat flux, and latent heat flux terms are plotted such that negative values denote loss of heat from the land surface or an upward flux. Thicker lines refer to a location near the storm center, while thinner lines are for a representative location in the outer reaches of the storm. (b) The surface ground temperatures are also shown for the corresponding locations.

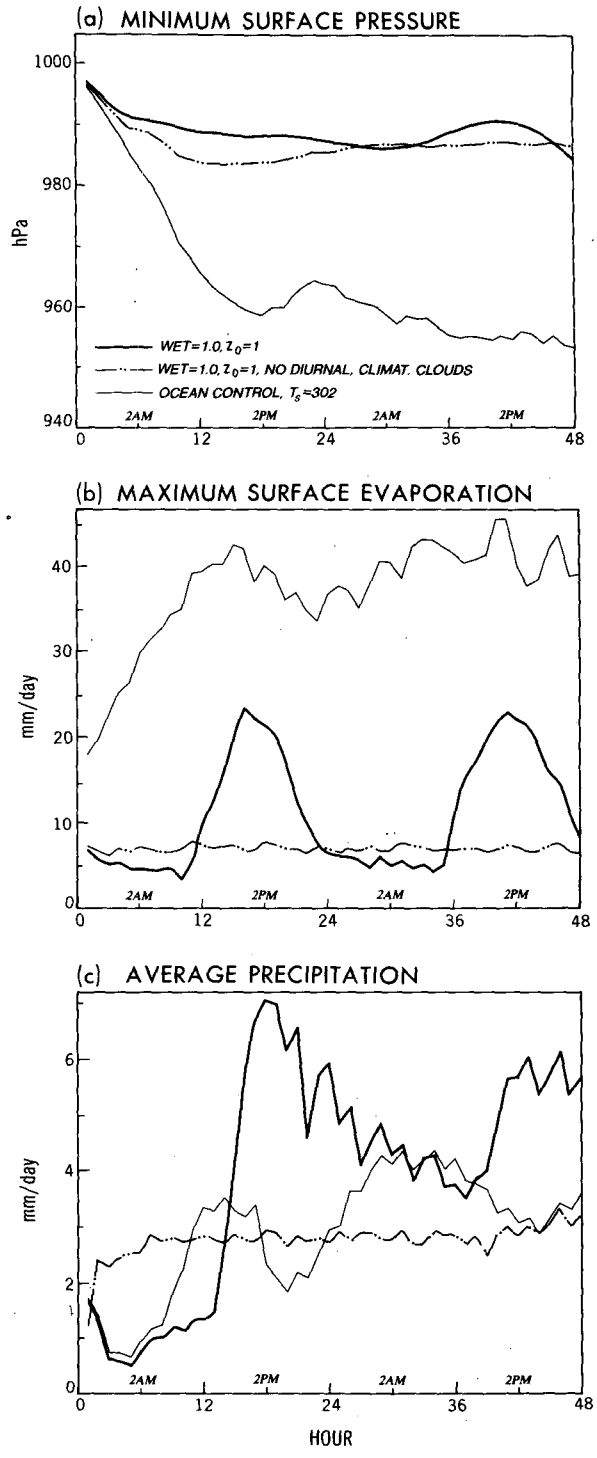

FIG. 6. (a) Minimum surface pressure, (b) maximum surface evaporation, and (c) domain average precipitation for a series of three experiments. In one case the land conditions were for evaporation set to the potential rate (i.e., WET = 1) and roughness length z_0 = 1 cm (thick solid line). In the second experiment a diurnally averaged solar flux was incorporated with zonally fixed, noninteracting clouds (dashed–dotted line) with otherwise identical land conditions. The third experiment is the ocean control case with specified SST = 302 K (thin solid line).

case the afternoon and evening precipitation maximum is highly correlated with the maximum value of convective available potential energy (CAPE), which exhibits a pronounced diurnal variability as well. On the other hand, the diurnal variation of CAPE over the ocean is small but out of phase with the precipitation variation shown in Fig. 6c. This seems consistent with the work of Duvel (1989), who indicated that it is primarily the diurnal warming of the surface and lower troposphere that drives the diurnal cycle of convection over a tropical landmass. For a region 8° × 8° surrounding the disturbance, the average CAPE is roughly the same (1100 J kg^{-1}) for the two days of integration for both land and ocean experiments. It is only in the inner 2° core region where CAPE is reduced to about 500 J kg^{-1} for the land case. This is a result of the cold pool beneath the disturbance. It is difficult to estimate the role of this reduced CAPE in the lack of develop-

ment. The topic of the diurnal variability of the tropical convection in the ocean control case and its relationship with observed variation of tropical convection is left for further study. However, one may speculate that the sometimes observed double precipitation maximum over oceans may be due to different mechanisms: one responsible for an early morning maximum as modeled here and observed by Gray and Jacobson (1977), and another mechanism responsible for the observed afternoon rainfall maximum (e.g., Duvel 1989) possibly associated with the maximum CAPE occurring in the afternoon over the ocean in the present model.

In summary, it appears that although diurnal variations and cloud feedback have an obvious impact on the hydrologic quantities of precipitation and evaporation the overall development potential of tropical disturbances over land is impeded even when diurnally averaged, fixed cloud conditions are assumed.

4. Impact of surface conditions at landfall

To assess the role of surface conditions on the phenomenon of landfall, a series of experiments similar to those in the previous section was performed. As mentioned in section 2, the experiments were designed with the same experimental framework and initial conditions as the all-land experiments except land conditions were specified for the surface west of 72°W with ocean conditions east of 72°W. For comparability purposes, the all-ocean case described previously was extended to 96 h. Experiments were designed in order that landfall will be at about 72 h (2000 LST). The land conditions were specified identically to those of section 3b and are shown in Table 1 (lower).

a. Effect of wetness, roughness, and T_L formulation

The relative importance of surface wetness, roughness, and surface temperature formulation was found to be similar in the landfall process as in the development process described in section 3. One sees that even for potentially wet (WET = 1) and smooth (z_0 = 1 cm) conditions a rapid decrease of intensity occurs at landfall. As indicated in Fig. 7, the low-level winds decrease by 20 m s^{-1} and surface pressure fills more than 30 hPa in a 36-h period. When the relative wetness is reduced by reducing WET to 0.3, a small further reduction of the storm intensity occurs with central surface pressures being 5 hPa higher. Little difference is noted in the reduction of maximum low-level winds. For the experiment with increased roughness, additional filling occurs, with a more dramatic further decrease in low-level winds (15 m s^{-1}). The abrupt reduction in surface sustained winds has been observed by Powell (1982) for landfalling storms. However, the winds aloft can be sustained for a much longer time and distance inland after landfall, which will be shown later. For the case with z_0 = 25 cm, the filling rate of 36 hPa (12 h)$^{-1}$ is consistent with observational and previous modeling studies (Tuleya et al. 1984). Also noteworthy is the small intensity increase in the late afternoon and evening (i.e., in the last 6 h of the experiments), which is analogous to a similar increase in the all-land experiments and may be attributed to increased afternoon convective activity and the delayed effect of increased daytime surface energy fluxes over the land. As will be shown in the next section, the landfall decay process is basically attributable to the effective cutoff of surface energy fluxes brought about by the

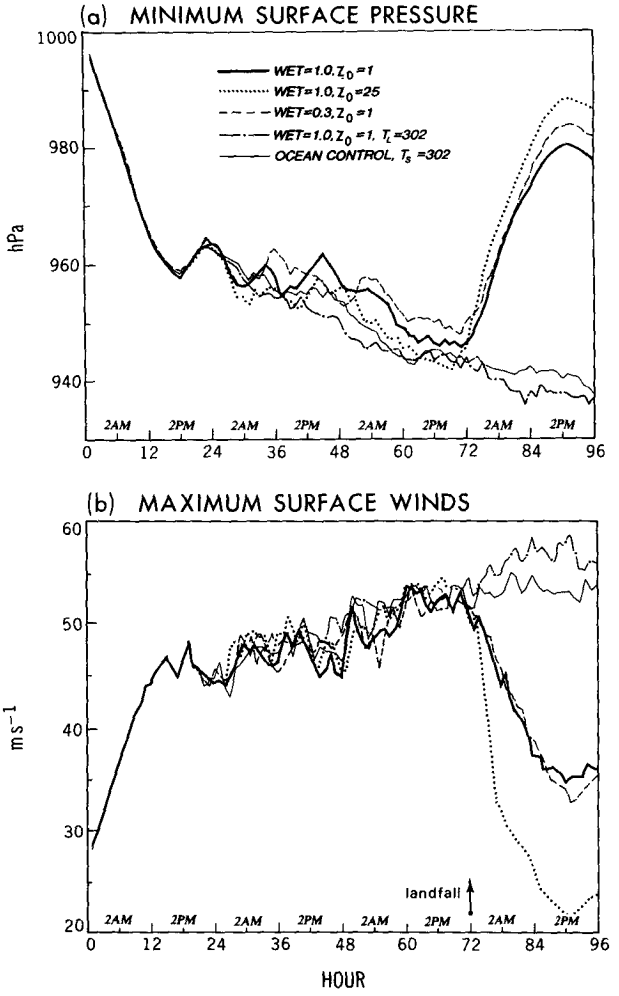

FIG. 7. (a) Minimum surface pressure and (b) maximum surface winds for a series of four experiments involving landfall are contrasted to an ocean control case (thin solid). In analogy to those experiments of Fig. 2, surface wetness (dashed line) and roughness (dotted line) are separately altered in two experiments from an experiment with potential evaporation (WET = 1) and roughness of 1.0 cm (thick solid). In a third experiment (dashed-dotted), land conditions are specified except the surface land temperature is fixed at 302 K. In the landfall experiments, land conditions including surface albedo, subsurface thermal property, roughness, and relative wetness are specified for all regions west of 73°W.

reduction of ground surface temperature as the hurricane comes ashore.

In an analogous manner to one of the experiments of section 3b, a model tropical cyclone failed to decay upon encountering a potentially wetland condition if the land surface T_L was fixed to 302 K. This has been shown previously by Tuleya and Kurihara (1978). It can be inferred from this series of experiments that realistic landfall decay occurs for a wide range of relative surface wetnesses and that surface roughness contributes but is not necessary in explaining the landfall decay process. To study the landfall process in more detail, the experiment with $z_0 = 25$ cm and evaporation prescribed at the potential rate will be examined in the next two sections.

b. *Reduction of surface energy flux and surface temperature*

As in section 3c, one can look at the surface energy flux as an indicator of the cause of the decay. As stated earlier, previous modeling studies have either a priori eliminated evaporation over land or arbitrarily reduced the surface temperature to a fixed value colder than the ocean. In the present experiments where surface temperature is explicitly predicted there is an abrupt reduction of 96-h accumulated evaporation at the coastline at the point of landfall with values of 6×10^7 J m^{-2} not penetrating over the land (Fig. 8). To first approximation, this result supports previous assumptions of zero evaporation over land. On the other hand, the evaporation in the environment surrounding the storm actually increases as evidenced by the values of 2×10^7 J m^{-2} expanding outward over land from the coastline. This may be a combined effect of increased daytime surface temperature together with increased surface roughness over land. Because of the high surface winds over the land near the coast and the reduction of ground surface temperature at landfall, there is an accompanying abrupt reversal of sensible heat flux from upward over the ocean to downward over the land. This effect, opposite to that of surface evaporation, acts to warm the surface immediately below the cyclone track. Over the ocean the latent energy flux is about seven times that of the sensible heat flux, while inland these two terms approximately balance as the storm passes.

The reduction of energy fluxes can be attributed to the lowering of ground temperature and the corresponding cool pool of surface air temperature beneath the landfalling storm. The lower surface temperature has been well known since Miller's (1964) work and confirmed by the recent work of Powell (1987). This was not well simulated in the modeling of tropical storm landfall to date (e.g., Tuleya et al. 1984), because of the physically unrealistic surface assumptions. Note in Fig. 9a and Fig. 9b the abrupt reduction in surface land temperature at the coast and a reduced T_L to below

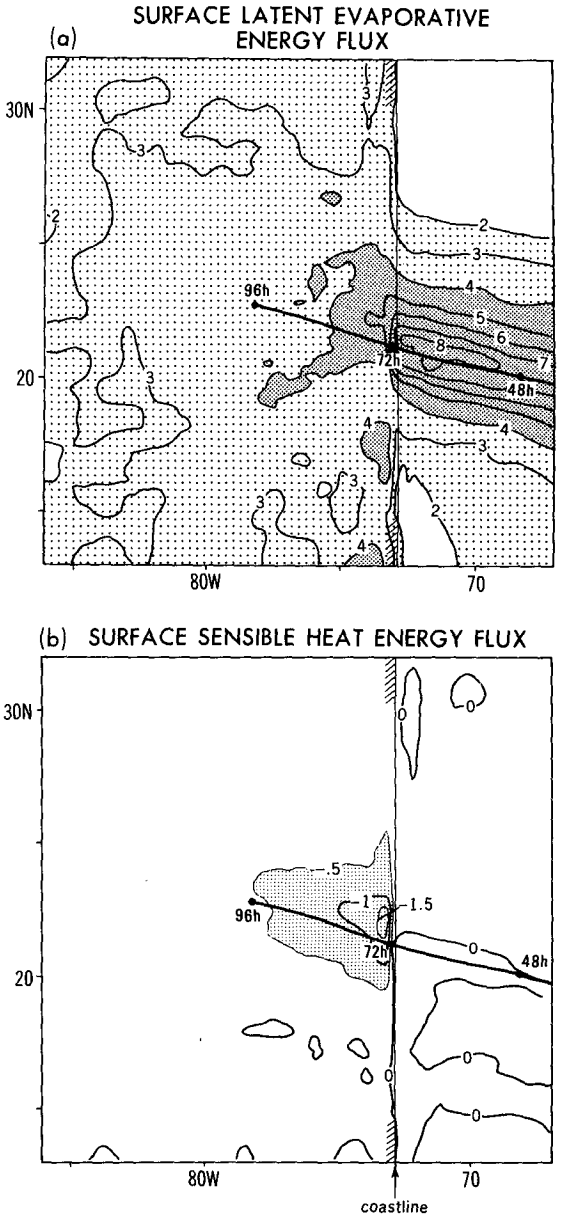

FIG. 8. (a) Total accumulated surface latent evaporative energy flux and (b) sensible heat flux for the landfall experiment for evaporation set to the potential rate (i.e., WET = 1) and roughness length $z_0 = 25$ cm. Units are 10^7 J m^{-2} for the 96-h integration period with storm track and 24-h position indicated for both experiments. Values greater than 2×10^7 and 4×10^7 J m^{-2} of evaporative energy flux are lightly and darkly shaded, respectively. Significant negative values less than -0.5×10^7 J m^{-2} of sensible heat flux are also shaded.

296 K and dry region of about 17 g kg^{-1} near the storm center 12 h after landfall (about 0800 LST). The corresponding θ_e distribution is shown in Fig. 9c and indicates low values of θ_e below 344 K near the landfalling storm. There is good correspondence between this field and observations of Powell (1987). This can be contrasted with values of greater than 360 K in the ocean

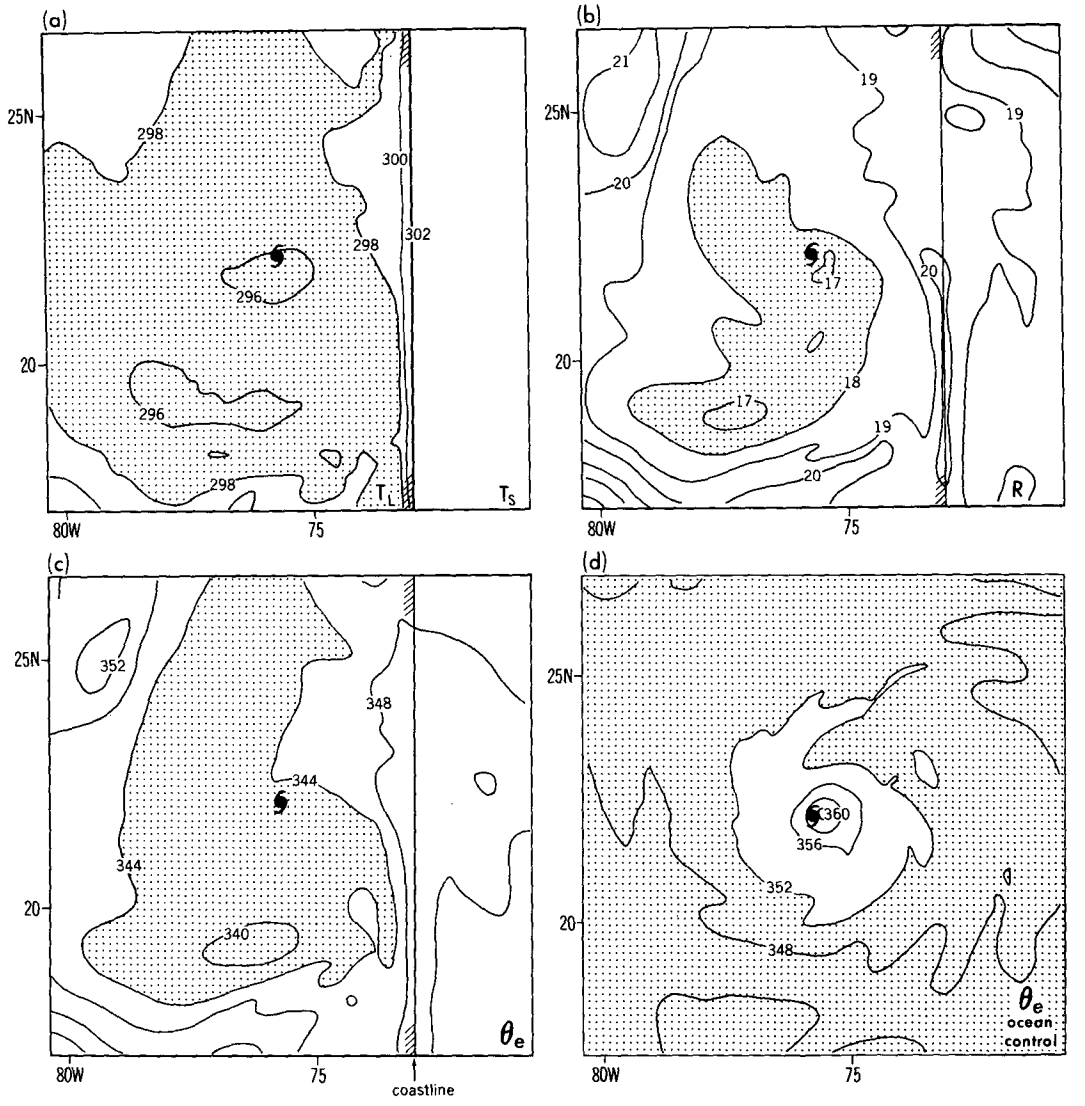

FIG. 9. (a) Composite distribution near and surrounding the disturbance of land temperature, (b) low-level mixing ratio, and (c) equivalent potential temperature for the landfall case with evaporation at the potential rate and roughness length set to 25 cm at 12 h after landfall (about 0800 LST). (d) The corresponding distribution of equivalent potential temperature of the ocean control experiment is also shown. The shaded areas indicate relatively cool and/or dry areas. The coastline for the landfall case is shown at 73°W.

control case, which is quite typical for observed tropical cyclones. Miller (1964) was the first to contrast the significant difference of low-level θ_e before and after hurricane landfall. In the present experiments, the surface temperature difference between storm and surroundings is more dramatic during daytime and concurs with observations by Bluestein (1989). This phenomenon is caused by the moderating effect of the cloudy canopy and is the result of the relative reduction of the net downward radiative surface flux during the day and its relative increase at night as discussed in section 3c. In a supplementary experiment not described in Table 1, a landfall case was performed without the radiative effect of clouds. In this experiment the cool surface temperature anomaly observed after landfall beneath the storm at 1400 LST was reduced 2.5 K relative to the interactive clouds case. The small diurnal variation in storm intensity after landfall as described in section 4a (Fig. 7) is slightly enhanced in magnitude and is more in phase with the solar heating in the no-clouds case. Therefore, the landfalling storm fills more rapidly at night (immediately after landfall) and reintensifies earlier (closer to time of maximum solar heating). To first approximation, however, the difference in experiments with and without clouds is rather minor with the maximum winds never being

more than 5 m s^{-1} different. For all landfall experiments there is a gradual decrease in the precipitation after landfall as shown in previous modeling studies, although some regions exist with amounts greater than 20 cm 400 km inland. This can be compared to rainfall maximum of about 30 cm before landfall and in the ocean control case. Dastoor and Krishnamurti (1991) have studied the sensitivity of various surface moisture parameterizations on improving rainfall forecasts at landfall using a specific case during the First GARP (Global Atmospheric Research Program) Global Experiment year.

c. *Wind field*

The discontinuity of low-level sustained wind speed at the coastline has been well documented through observations (Powell 1982, 1987) and modeling (Tuleya et al. 1984). One may look at a swath of maximum wind similar to that of Fujita (1980) for the idealized landfalling experiment with WET = 1 and z_0 = 25 cm and note this abrupt discontinuity (Fig. 10a). The low-level model hurricane-force winds penetrate approximately 150 km inland, which can be compared to 132 and 230 km for Hurricanes Camille (1969) and Fredric (1979). Model winds can be interpreted as analogous to observations of sustained winds. One would anticipate that surface gusts be significantly higher and may be correlated with wind fields aloft (Powell 1982). In this idealized experiment, hurricane-force winds at the top of the boundary layer survive to the end of the integration near the storm with only a gradual reduction occurring in the peak winds of 70 m s^{-1} at landfall to below 50 m s^{-1} 500 km inland (Fig. 10b). In contrast to simulations with topographical influences (e.g., Bender et al. 1987), little deflection occurs in track in this simulation. Before landfall the storm position was never more than 15 km from that of the ocean control case. After landfall, the storm appears to speed up about 1 m s^{-1} for the first 12–18 h and then decelerates. The final 96-h position is within 40 km of that of the ocean control case.

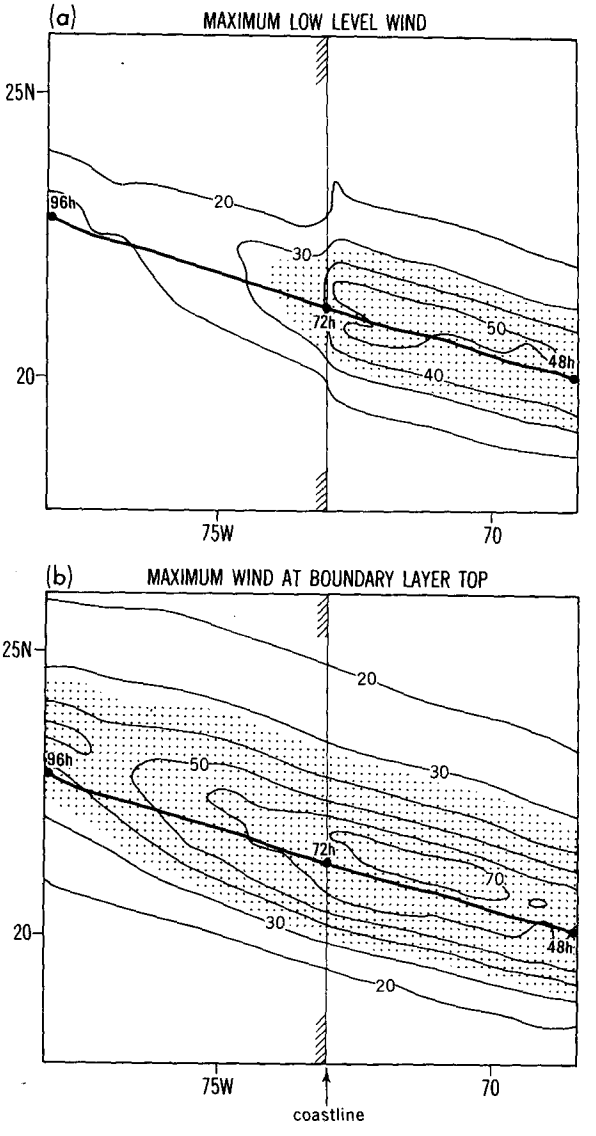

FIG. 10. (a) Horizontal distribution of maximum low-level (σ = 0.995) wind and (b) maximum wind at the boundary-layer top (σ = 0.9204) during tropical storm passage for the landfall case with evaporation at the potential rate and roughness set to 25 cm. Storm tracks are shown with 24-h positions indicated. Shading indicates hurricane-force winds (>33 m s^{-1}). Land is to the west of the indicated coastline at 73°W.

5. Summary and conclusions

The question of why tropical cyclones do not develop extensively over land has been studied through a series of sensitivity experiments with identical atmospheric but various land surface initial conditions. The modeling basis for these simulations has been made more physically realistic through the inclusion of a bulk subsurface layer and radiation parameterization into the GFDL MMM where surface land temperatures are explicitly predicted. It was discovered that an otherwise cyclogenic initial condition for ocean conditions failed to develop to any significant intensity for typical land conditions, even with evaporation specified at the potential rate. It was found that evaporation, the prime source of energy of tropical cyclones, was significantly retarded, without its explicit cutoff, as has typically been assumed in previous model simulations. In this model the evaporation was significantly reduced over land due to the finite heat capacity and conductivity of the soil subsurface allowing a reduction of the ground temperature beneath the incipient storm. This has the dramatic impact of reversing the known positive feedback between low-level winds and evaporation in increasing the development rate of tropical cyclogenesis. Associated with this reduced evaporation and minimum

ground surface temperature is a relative low-level minimum in θ_e near the disturbance center, opposite to that which occurs in tropical cyclones over the ocean. It was found that the cloud canopy reduces the net downward radiation during the day beneath the disturbance but increases the downward flux at night. This leads to the model result that the cool pool of surface air and ground temperature in the storm core region is largest during the day.

It was found that the thermal property of the subsurface (i.e., the combined effect of soil heat capacity and conductivity) had a dramatic influence on the development or lack of development of the tropical cyclone. Experiments with characteristic values typical of soil lead to a lack of significant development, but an experiment with a value similar to that of a mixed ocean layer leads to a development similar to that of an ocean control case. It was also found that the hydrologic cycle was different over land and ocean, with the diurnal cycle of precipitation and evaporation more pronounced for experiments with land conditions. There were no dramatic impacts of the diurnal cycle and cloud variation on the overall intensity of the disturbance over land, although the large-scale budgets of moisture and heat were affected. An interesting ocean precipitation maximum occurred in late evening and early morning that was negatively related to the ambient CAPE. The precipitation over land occurred during late afternoon (1400–2000 LST) and was positively related to surface heating and corresponding large values of CAPE.

In sensitivity experiments analogous to the all-land cases, similar mechanisms were found active in a series of landfall simulations. Even when evaporation was prescribed at the potential rate, rapid filling ensued similar to observed scenarios. Results indicated a low-level cooling, an abrupt discontinuity of surface model winds, and a highly impeded evaporation rate beneath the landfalling disturbance. Variations in surface albedo and roughness do not significantly affect landfalling storm intensity if the surface ground temperature remains artificially high for potentially wet conditions. However, surface roughness and reduced relative wetness do contribute to enhanced decay. For landfalling simulations, it was found that precipitation and upper-level winds were both more gradually reduced as the hurricane moves inland. Some regions of intense boundary-layer winds and high rainfall occur well inland. These results are quite realistic considering the idealized nature of the simulations that do not account for topographical influences or extratropical interactions.

This leads to the conclusion that the rapid filling of a tropical cyclone at landfall is due to the reduction of surface ground temperature beneath the storm, which is due in turn to the finite heat capacity and conductivity of the soil subsurface layer. Again, as in the all-land case, the demise of the landfalling storm takes place due to the suppression of the potential evaporation and the associated reduction of surface air and land temperatures beneath the landfalling cyclone. The present landfalling experiments tend to support previous hurricane modeling assumptions that have a priori eliminated surface energy fluxes over land.

The results of these simulations tend to support the GFDL MMM regional model capabilities in forecasting and simulating situations over land when a bulk ground-level temperature formulation and radiation scheme with interactive clouds are included in the model physics. Recent research has reevaluated the role of an interactive ocean in accurately forecasting storm intensity and track. In the future, further improvements in ocean interaction, cloud specification, and, perhaps, surface hydrology will be considered. In addition, the present model simulations have also uncovered interesting diurnal and cloud interaction effects that may be important for tropical simulations of both short and long time scales. This demands further investigation.

Acknowledgments. The author would like to thank J. Mahlman, GFDL director, and Y. Kurihara, project head, for their continuous support for this investigation. L. Donner and Y. Kurihara read an earlier version of this manuscript and provided constructive criticism. The author also benefited from discussions on tropical disturbances in GCMs with S. Manabe and A. Broccoli. M. Bender supplied the initial conditions, while D. Schwarzkopf and W. Stern aided in implementing the Fels–Schwarzkopf radiation package into the GFDL tropical cyclone model. Credit is also given to P. Tunison, K. Raphael, and J. Varanyak for drafting assistance.

REFERENCES

Bender, M. A., R. E. Tuleya, and Y. Kurihara, 1985: A numerical study of the effect of a mountain range on a landfalling tropical cyclone. *Mon. Wea. Rev.*, **113**, 567–582.

——, ——, and ——, 1987: A numerical study of the effect of island terrain on tropical cyclones. *Mon. Wea. Rev.*, **115**, 130–155.

——, I. Ginis, and Y. Kurihara, 1994: Numerical simulations of the tropical cyclone–ocean interaction with a high resolution coupled model. *J. Geophys. Res.*, **98**, in press.

Bengtsson, L., H. Bottger, and M. Kanamitsu, 1982: Simulation of hurricane-type vortices in a general circulation model. *Tellus*, **34**, 440–457.

Bluestein, H. B., and D. S. Hazen, 1989: Doppler-radar analysis of a tropical cyclone over land; Hurricane Alicia (1983) in Oklahoma. *Mon. Wea. Rev.*, **117**, 2594–2611.

Broccoli, A. J., and S. Manabe, 1990: Can existing climate models be used to study anthropogenic changes in tropical cyclone climate? *Geophys. Res. Lett.*, **17**, 1917–1920.

Dastoor, A., and T. N. Krishnamurti, 1991: The landfall and structure of a tropical cyclone: The sensitivity of model predictions to soil moisture parameterizations. *Bound.-Layer Meteor.*, **55**, 345–380.

Deardorff, J. W., 1978: Efficient prediction of ground surface temperature and moisture, with inclusion of a layer of vegetation. *J. Geophys. Res.*, **83**, 1889–1903.

Duvel, J. P., 1989: Convection over tropical Africa and the Atlantic ocean during northern summer: Part I. Interannual and diurnal variations. *Mon. Wea. Rev.*, **117**, 2782–2799.

Emanuel, K. A., 1988: Toward a general theory of hurricanes. *Amer. Sci.*, **76,** 371–379.

Evans, J. L., 1992: Comment on "Can existing climate models be used to study anthropogenic changes in tropical cyclone climate." *Geophys. Res. Lett.*, **19,** 1523–1524.

Fujita, T. T., 1980: In search of mesoscale wind fields in landfalling hurricanes. *Proc. 13th Conf. on Hurricanes and Tropical Meteor.*, Miami Beach, FL, Amer. Meteor. Soc., 43–57.

Gray, W. M., and R. Jacobson, 1977: Diurnal variation of deep cumulus convection. *Mon. Wea. Rev.*, **105,** 1171–1188.

Hawkins, H. F., and S. M. Imbembo, 1976: The structure of a small, intense hurricane, Inez 1966. *Mon. Wea. Rev.*, **104,** 418–442.

Krishnamurti, T. N., D. Oosterhof, and N. Digon, 1989: Hurricane prediction with a high resolution global model. *Mon. Wea. Rev.*, **117,** 631–666.

Kurihara, Y., and R. E. Tuleya, 1974: Structure of a tropical cyclone developed in a three-dimensional numerical simulation model. *J. Atmos. Sci.*, **31,** 893–919.

——, and ——, 1981: A numerical simulation study on the genesis of a tropical storm. *Mon. Wea. Rev.*, **109,** 1629–1653.

——, M. A. Bender, R. E. Tuleya, and R. Ross, 1993: Hurricane forecasting with the GFDL automated prediction system. *Proc. 20th Conf. on Hurricanes and Tropical Meteor.*, San Antonio, TX, Amer. Meteor. Soc., 323–326.

Lacis, A. A., and J. E. Hansen, 1974: A parameterization for the absorption of solar radiation in the earth's atmosphere. *J. Atmos. Sci.*, **31,** 118–133.

London, J., 1957: A study of the atmospheric heat balance. Final report. AFCRC Contract AF19122-165, New York University, 99 pp.

Manabe, S., and J. Smagorinsky, 1967: Simulated climatology of a general circulation model with a hydrologic cycle. *Mon. Wea. Rev.*, **95,** 155–169.

——, J. L. Holloway, and H. M. Stone, 1970: Tropical circulation in a time integration of a global model of the atmosphere. *J. Atmos. Sci.*, **27,** 580–613.

Mathur, M. B., 1991: The national meteorological center's quasi-lagrangian model for hurricane prediction. *Mon. Wea. Rev.*, **119,** 1419–1447.

McBride, J. L., 1984: Comments on "Simulation of hurricane-type vortices in a general circulation model." *Tellus*, **36A,** 92–93.

Miller, B., 1964: A study of the filling of hurricane Donna (1960). *Mon. Wea. Rev.*, **92,** 389–406.

Ooyama, K. V., 1969: Numerical simulation of the life cycle of tropical cyclones. *J. Atmos. Sci.*, **26,** 3–40.

Powell, M. D., 1982: The transition of the hurricane Fredric boundary wind field from the open Gulf of Mexico to landfall. *Mon. Wea. Rev.*, **110,** 1912–1932.

——, 1987: Changes in the low-level kinematic and thermodynamic structure of hurricane Alicia (1983) at landfall. *Mon. Wea. Rev.*, **115,** 75–99.

Rosenthal, S., 1971: The response of a tropical cyclone model to variations in boundary layer parameters, initial conditions, lateral boundary conditions and domain size. *Mon. Wea. Rev.*, **99,** 767–777.

Schwarzkopf, M. D., and S. B. Fels, 1991: The simplified exchange method revisited: An accurate, rapid method for computation of infrared cooling rates and fluxes. *J. Geophys. Res.*, **96,** 9075–9096.

Sellers, W. D., 1967: *Physical Climatology.* The University of Chicago Press, 272 pp.

Tuleya, R. E., 1988: A numerical study of the genesis of tropical storms observed during the FGGE year. *Mon. Wea. Rev.*, **116,** 1188–1208.

——, and Y. Kurihara, 1978: A numerical simulation of the landfall of tropical cyclones. *J. Atmos. Sci.*, **35,** 242–257.

——, M. A. Bender, and Y. Kurihara, 1984: A simulation study of the landfall of tropical cyclones using a movable nested-mesh model. *Mon. Wea. Rev.*, **112,** 124–136.